USCAP

www.nature.com/labinvest

ARTICLE

Check for updates

Nobiletin protects retinal ganglion cells in models of ocular hypertension in vivo and hypoxia in vitro

Dan-Dan Wang[1,2,3], Feng-Juan Gao[1,2,3], Xue-Jin Zhang[1,2,3], Fang-Yuan Hu[1,2,3], Ping Xu[1,2,3] and Ji-Hong Wu[1,2,3]✉

Glaucoma, a common cause of blindness, is characterized by the progressive loss of retinal ganglion cells (RGCs). Growing evidence suggests that nobiletin (NOB) is a promising neuroprotective drug; however, its effects on glaucomatous neurodegeneration remain unknown. Using rat models of microbead occlusion in vivo and primary RGCs model of hypoxia in vitro, we first demonstrate that NOB reduces RGC apoptosis by a TUNEL assay, Hoechst 33342 staining and FluoroGold (FG) retrograde labeling. This effect does not depend on intraocular pressure (IOP) lowering. Additionally, NOB partially restored the functional and structural damage of inner retinas, attenuated Müller glial activation and oxidative stress caused by ocular hypertension. At 2 weeks after IOP elevation, NOB further enhanced Nrf2/HO-1 pathway in RGCs to withstand the cumulative damage of ocular hypertension. With the administration of HO-1 inhibitor tin-protoporphyrin IX (SnPP), the protective effect of NOB was attenuated. Overall, these results indicate that NOB exerts an outstanding neuroprotective effect on RGCs of glaucomatous neurodegeneration. Besides, interventions to enhance activation of Nrf2/HO-1 pathway can slow the loss of RGCs and are viable therapies for glaucoma.

Laboratory Investigation (2022) 102:1225–1235; https://doi.org/10.1038/s41374-022-00813-8

INTRODUCTION

Glaucoma, a main cause of irreversible blindness worldwide[1], is characterized by the death of retinal ganglion cells (RGCs) and axon degeneration. Currently, intraocular pressure (IOP) reduction is the main therapy for glaucoma; however, even when IOP is returned to a normal range, optic nerve damage continues in some patients[2,3]. Thus, there is an urgent need for safe and effective neuroprotective strategies for the treatment of glaucoma. Increasing evidence supports a role for oxidative stress in the degeneration of RGCs and the pathogenesis of glaucoma[4,5]. The cellular response to oxidative stress is regulated in part by a signaling pathway that culminates in activation of the transcription factor nuclear factor erythroid 2-related factor 2 (Nrf2) and transcription of its antioxidant target genes. As such, Nrf2 has been proposed as a potential therapeutic target for glaucoma[6,7]. Under normal conditions, Nrf2 is sequestered in the cytoplasm by binding to Kelch-like ECH associated protein 1 (Keap1), a ubiquitin ligase adaptor protein that regulates Nrf2 stability by targeting it for degradation. However, under conditions of oxidative stress, Keap1 undergoes a conformational change and releases Nrf2 into the cytoplasm; Nrf2 then translocates to the nucleus and activates the expression of a range of antioxidant proteins, including heme oxygenase 1 (HO-1)[8]. In this study, we focus on the Nrf2/HO-1 signaling pathway, and aim to better understand the molecule mechanisms in the process of glaucoma.

Nobiletin (NOB) is the main polymethoxylated flavone in citrus fruits and is especially abundant in the peel[9]. NOB has been shown to have multiple potentially beneficial properties and has received increasing attention as a therapeutic agent for various diseases. Several studies have shown that NOB can improve mitochondrial dysfunction and alleviate endoplasmic reticulum stress[10,11]. In addition, NOB was reported to ameliorate synaptic dysfunction in mice with lipopolysaccharide-induced memory deficiency[12]. NOB was shown to be an agonist of retinoid acid receptor-related orphan receptor, and through this mechanism potentiated circadian oscillation and optimized mitochondrial respiration in skeletal muscle, thereby promoting the healthy aging[13]. Notably, the antioxidant and anti-inflammatory properties of NOB suggest that it may have neuroprotective potential for the treatment of Alzheimer's disease and Parkinson's disease[14,15], and, possibly, other neurodegenerative disorders. However, whether or how NOB may have utility for the treatment of glaucoma is still unknown.

Here, we tested our hypothesis that NOB may be neuroprotective by employing a microbead occlusion-induced model of ocular hypertension (OHT) in rats and exposure of RGCs to hypoxia in vitro to mimic conditions associated with glaucoma. We found that NOB enhances RGC survival, independently of lowering of IOP, in a manner associated with reduced retinal oxidative stress and inhibition of Müller glial activation. Moreover, NOB relieved oxidative stress in this model *via* activation of the Nrf2/HO-1 pathway. This is the first report of the protective effects of NOB and its underlying mechanism of action in glaucomatous neurodegeneration, and our results indicate that the Nrf2/HO-1 pathway may be a feasible therapeutic target for glaucoma.

[1]Eye Institute, Eye and ENT Hospital, College of Medicine, Fudan University, Shanghai, China. [2]Shanghai Key Laboratory of Visual Impairment and Restoration, Science and Technology Commission of Shanghai Municipality, Shanghai, China. [3]Key Laboratory of Myopia, Ministry of Health, Shanghai, China. ✉email: jihongwu@fudan.edu.cn

Received: 13 April 2022 Revised: 29 May 2022 Accepted: 30 May 2022
Published online: 8 July 2022

MATERIALS AND METHODS

Cultured RGC studies

All animal experiments were performed in compliance with the Association Research in Vision and Ophthalmology Statement for the Use of Animals in Ophthalmic and Vision Research, and were approved by the Animal Experimental Ethics Committee of the Eye and ENT Hospital of Fudan University. RGCs were obtained from newborn Sprague-Dawley rats (3 days) and were dissociated, purified and cultured as previously described[16]. After 48 h of seeding, RGCs were exposed to hypoxic conditions (3% O_2, 92% N_2, 5% CO_2) with or without NOB at 37 °C for another 48 h to induce hypoxic injury and apoptosis. The apoptosis of RGCs were measured by a TUNEL assay and Hoechst 33342 staining, as previously reported[17].

Animals and rat models of ocular hypertension

Adult male Wistar rats (200–250 g) were obtained from the Shanghai Laboratory Animal Center Co., Ltd. The rats were housed in standard cages with a 12-h light/dark cycle and were given free access to standard rodent diets and water.

The OHT model was induced by injection of 8 μL superparamagnetic microspheres (Bangs Laboratories, Fishers, IN, USA; 10 μm diameter) into the anterior chamber as previously described[18]. In parallel, a sham-operated control group of rats were injected with the same volume of saline. IOP was measured in both eyes before surgery and at 3 days and 1, 2, 3, and 4 weeks after surgery using a Tonolab tonometer (Icare, Helsinki, Finland). All IOP measurements were performed by the same operator between 9 a.m. and 10 a.m., and each value represents the average of six valid measurements. The eyes receiving microspheres injection were considered to be successfully induced when their IOP increased by more than 5 mmHg compared with the control eyes[19], and they were excluded from further experiment if IOP returned to normal.

Intravitreal injections

OHT rats undergo intravitreal injection of 3 μL of vehicle or 10 μM nobiletin (NOB; MedChemExpress, NJ, USA) and/or 20 μM tin-protoporphyrin IX (SnPP; MedChemExpress) before surgery and every 7 days thereafter. In brief, the pupils were dilated under anesthesia using 0.5% tropicamide and 0.5% phenylephrine hydrochloride eye drops, and the ocular surface was then anesthetized by addition of 0.4% oxybuprocaine hydrochloride eye drops. As previously described[20], intravitreal injection was performed using a 10 μL Hamilton syringe connected to a 30-gauge needle.

Retrograde labeling and quantification of RGCs

Methanesulfonate (3%, diluted in 10% dimethyl sulfoxide saline), known as FluoroGold (FG), was purchased from Sigma–Aldrich (St. Louis, MO, USA). As previously reported[21], the rats were anesthetized and 2 μL FG was injected into both superior colliculi 1 week before euthanasia. After euthanasia, the eyes were obtained and fixed in 4% paraformaldehyde at room temperature for 1.5 h. Then the retinas were carefully separated and processed into flat mounts. Images of retinas were photographed using a Leica DMI 3000B microscope. To count the number of RGCs, each retina was divided into four quadrants, each of which was further divided into central (1–2 mm from the optic disc), middle (2–3 mm from the optic disc) and peripheral regions (3–4 mm from the optic disc). In total, RGCs in 12 microscopic fields per retina were independently counted using ImageJ software by two experimenters who were blinded to the experimental grouping. Data are shown as the mean number of RGCs per mm^2.

TdT-mediated dUTP nick end labeling (TUNEL) assay

Apoptosis of RGCs was measured using a TdT-mediated dUTP nick end labeling (TUNEL) assay (In Situ Cell Detection Kit, TMR red; Roche, Mannheim, Germany) according to the manufacturer's protocol. Subsequently, apoptosis of RGCs in tissue sections and primary RGCs was additionally evaluated by staining of the cell nuclei with Hoechst 33258 and 4′6-diamidino-2-phenylindole (DAPI) dyes, respectively. Images were obtained with a Leica SP8 confocal microscope (×20). To count the number of TUNEL-positive cells, the ImageJ software was used to analyze 5 random fields of view in each slide, and the average values were calculated. The results are shown as the mean percentage of TUNEL-positive cells.

Hematoxylin-eosin (H&E) staining and immunohistochemistry

At 2 weeks post-surgery, the eyeballs were collected and sequentially fixed, paraffin embedded, sliced into 5-μm sections, deparaffined, and rehydrated as previously reported[19,22]. Then, H&E staining was performed to evaluate retinal damage, and 8-hydroxyguanosine (8-OHdG), a product of oxidative DNA damage, was detected by immunohistochemistry to evaluate retinal oxidative stress. Images were captured with a Leica light microscope and analyzed by ImageJ.

Photopic negative response (PhNR) recording

To evaluate the function of RGCs, PhNR was recorded at 2 weeks post-surgery[23]. In this study, we used a Diagnosys Espion System (Espion E2; Diagnosys, MA, USA) to provide the light stimulate and obtain the data. After pupil dilation and light adaptation for at least 10 min, the rats were placed on a blue background for brief preadaptation. A brief red stimulus at 10 cd/m^2 was then delivered through a Ganzfeld sphere on a blue background of 20 cd/m^2. The flash duration was 4 ms and the frequency was 0.5 Hz. Two 3-mm platinum wire loop electrodes were attached to the surface of cornea to record the responses. The ground electrode was placed on the tail, and the reference electrode was placed over the nasal bone. The amplitudes of PhNR was measured from prestimulus baseline to the trough following the b-wave.

Immunofluorescence

Eyeballs were collected, fixed, dehydrated, embedded, and sliced into 10-μm sections as previously described[24]. At room temperature, the sections were permeabilized with 0.1% Triton X-100 for 20 min, and subsequently blocked with 3% bovine serum albumin (BSA) for 1 h. Then they were incubated with rabbit anti-glial fibrillary acidic protein (GFAP) antibody (1:200; Cell Signaling Technology, Danvers, MA, USA) or rabbit anti-Nrf2 antibody (1:200; Abcam, Cambridge, UK) at 4 °C overnight. After washing with PBS for three times, the tissue sections were incubated with Alexa Fluor 488-conjugated goat anti-rabbit antibody (1:500, Cell Signaling Technology) or Alexa Fluor 555-conjugated donkey anti-rabbit antibody (1:800; Invitrogen, Carlsbad, CA, USA) at room temperature for 1 h. The cell nuclei were stained with Hoechst 33258 and the tissue sections were photographed with a Leica SP8 confocal microscopy.

Western blot analysis

Retinas were lysed with RIPA buffer (Beyotime, Shanghai, China) and smashed with ultrasound on ice, or proteins were extracted from retinas with a nuclear and cytoplasmic protein extraction kit according to the manufacturer's protocol (Beyotime). Then the protein concentration was quantified with a BCA protein assay kit (Beyotime). In each sample, equivalent amounts of protein were separated by polyacrylamide gel electrophoresis, and subsequently electrotransferred onto 0.22-μm polyvinylidene difluoride membranes. After blocking with 5% nonfat dry milk at room temperature for 1 h, the membranes were incubated with rabbit anti-GFAP antibody (1:1000, Cell Signaling Technology), rabbit anti-β-actin antibody (1:1000, Cell Signaling Technology), rabbit anti-Nrf2 antibody (1:1000, Abcam), rabbit anti-HO-1 antibody (1:1000, Cell Signaling Technology) or rabbit anti-histone H3 antibody (1:2000, Cell Signaling Technology) at 4 °C overnight. Then the membranes were incubated with horseradish-peroxidase-conjugated goat anti-rabbit IgG (1:2000, Cell Signaling Technology) at room temperature for 1 h after rinsing with 1× TBST for three times. Lastly, the signals were developed with a chemiluminescence detection kit (Thermo Fisher Scientific, CA, USA). The Kodak Imaging Station (Kodak 4000 MM PRO; Carestream, NY, USA) was used to capture the images which were analyzed by ImageJ. The results are expressed as the fold intensity relative to the control group.

Quantitative PCR

Total RNA was extracted from retinas, reverse transcribed into cDNA, and amplified by quantitative PCR as previously described[19]. The primer sequences for Nrf2, Keap1, HO-1, and β-actin were as described and verified in a previous study[25]. β-Actin was measured as the internal control, and assays were done in triplicate with 6 retinas.

Statistical analysis

All data are expressed as means ± SD. One-way analysis of variance and Tukey multiple comparisons test were performed in this study with

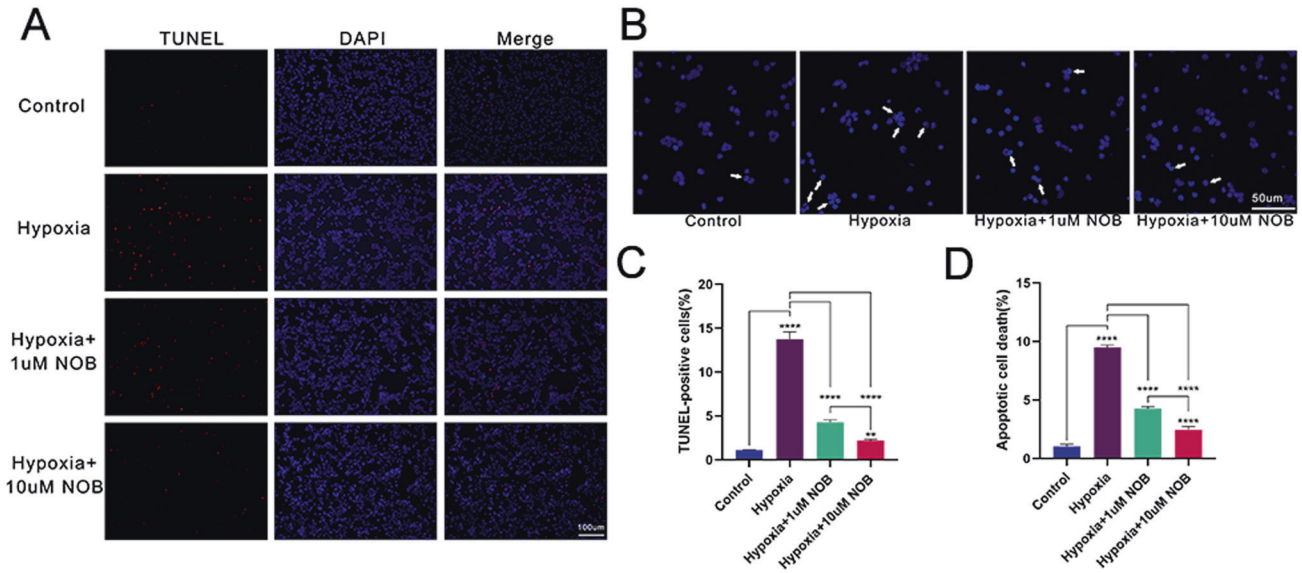

Fig. 1 NOB protects RGCs against apoptosis in vitro after 48 h of hypoxia. A Representative immunofluorescence images of RGCs stained with TUNEL and DAPI. Scale bar, 100 μm. **B** Representative immunofluorescence images of RGCs labeled with Hoechst 33342. Scale bar, 50 μm. **C** Quantitative analysis of TUNEL-positive cells. **D** Quantitative analysis of RGC apoptosis. The results are presented as mean ± SD, $n = 3$. ****$P < 0.0001$.

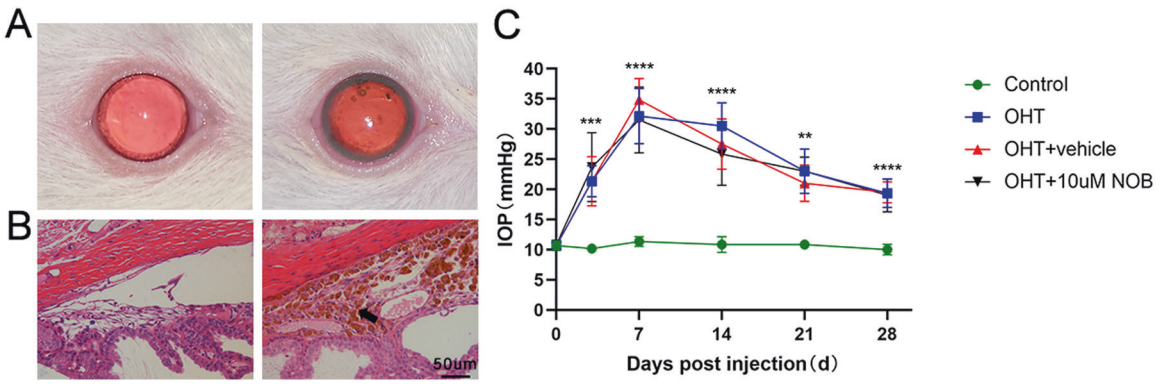

Fig. 2 NOB has no effect on IOP in rats with OHT. A Representative anterior segment photographs of control and ocular hypertensive rats. **B** Representative H&E staining images of anterior chamber angle in control and ocular hypertensive rats. Black arrow indicates the distribution of magnetic beads in the anterior chamber angle. Scale bar, 50 μm. **C** Changes in IOP before surgery and at 3 days and 1, 2, 3, and 4 weeks after surgery. The data are shown as mean ± SD, $n = 6$. **$P < 0.01$, ***$P < 0.001$ and ****$P < 0.0001$.

GraphPad Prism 8.0 (San Diego, CA, USA). A P value < 0.05 was considered statistically significant.

RESULTS

NOB reduces hypoxia-induced apoptosis of RGCs in vitro

Previous research has shown that oxidative stress and hypoxia play an important role in the pathogenesis of glaucoma[26]. In this study, RGCs were exposed to 3% O_2 for 48 h to induce apoptosis in vitro; a TUNEL assay and Hoechst 33342 staining were performed to measure the apoptosis of RGCs. As shown in Fig. 1, NOB treatment at 1 μM and 10 μM reduced hypoxia-induced cell apoptosis (all $P < 0.0001$, $n = 3$), with 10 μM NOB having the better protective effect ($P = 0.0017$ and $P < 0.0001$ by the TUNEL assay and Hoechst 33342 staining, respectively; $n = 3$). These results indicate that NOB protects RGCs against hypoxia-induced apoptosis in vitro. All subsequent experiments were performed using NOB at 10 μM.

NOB has no effect on IOP in a rat model of OHT

To investigate the effect of NOB on RGCs in vivo, the anterior chambers of Wistar rats were injected with microspheres to model the pathophysiology of glaucoma (Fig. 2A, B). IOP plays a critical role in glaucoma and is currently the main therapeutic target[27]. IOP was measured before surgery and then at 3 days and 1, 2, 3, and 4 weeks after surgery. As shown in Fig. 2C, no apparent difference was observed in baseline IOP among the four groups ($P = 0.9778$, $n = 6$). On day 3 after injection, IOP was significantly elevated compared with the control ($P = 0.0003$, $n = 6$), and the effect lasted until 4 weeks after surgery ($P < 0.0001$ at 1, 2, and 4 weeks, $P = 0.0025$ at 3 weeks; $n = 6$). Thus, microsphere injection successfully induced a sustained elevation in IOP. Notably, there was no significant difference in IOP between NOB group and vehicle group at any indicated time point within 4 weeks (all $P > 0.05$, $n = 6$), indicating that NOB administration had no effect on IOP in this rat model of OHT.

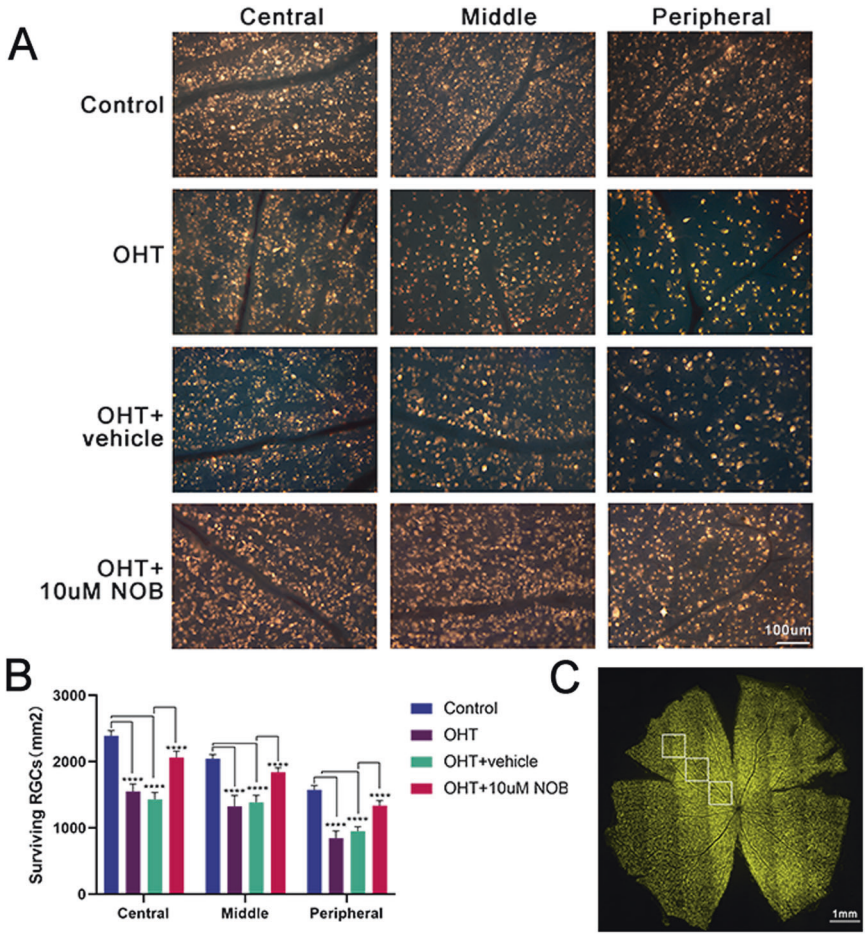

Fig. 3 NOB promotes RGC survival at 2 weeks post-IOP elevation. A Representative images of RGCs labeled with FG. Scale bar, 100 μm. **B** Quantitative analysis of surviving RGCs. **C** Whole flat-mounted retina from control rats. White boxes show the areas of RGCs counts. Scale bar, 1 mm. The results are expressed as mean ± SD, $n = 6$. ****$P < 0.0001$.

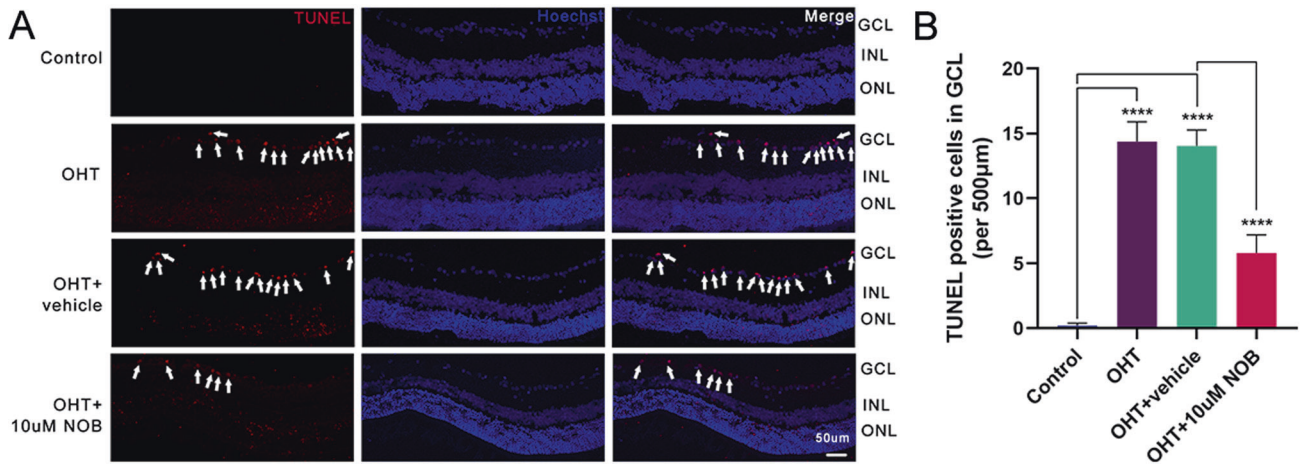

Fig. 4 NOB reduces RGC apoptosis at 2 weeks post-IOP elevation. A Representative immunofluorescence images of retinal sections labeled with TUNEL and Hoechst 33258. Scale bar, 50 μm. **B** Quantitative analysis of TUNEL-positive cells in the GCL. The results are presented as mean ± SD, $n = 6$. ****$P < 0.0001$.

NOB reduces RGC apoptosis in a rat model of OHT

RGCs have been reported to undergo apoptosis after 2 weeks of IOP elevation[28]. To explore the effect of NOB on RGC apoptosis in glaucomatous neurodegeneration, we counted the number of RGCs using FG retrograde labeling (Fig. 3C). As shown in Fig. 3A and B, the average RGC densities in control group were 2392 ± 80 cells/mm^2 in the central, 2046 ± 63 cells/mm^2 in the middle and 1577 ± 63 cells/mm^2 in the peripheral region. At 2 weeks after surgery, the rats in OHT group had a 35% RGCs loss in the central region ($P < 0.0001$, $n = 6$) and 35% in the middle region ($P < 0.0001$, $n = 6$) compared with the control. The peripheral retina suffered the most damage, with a 46% loss of RGCs

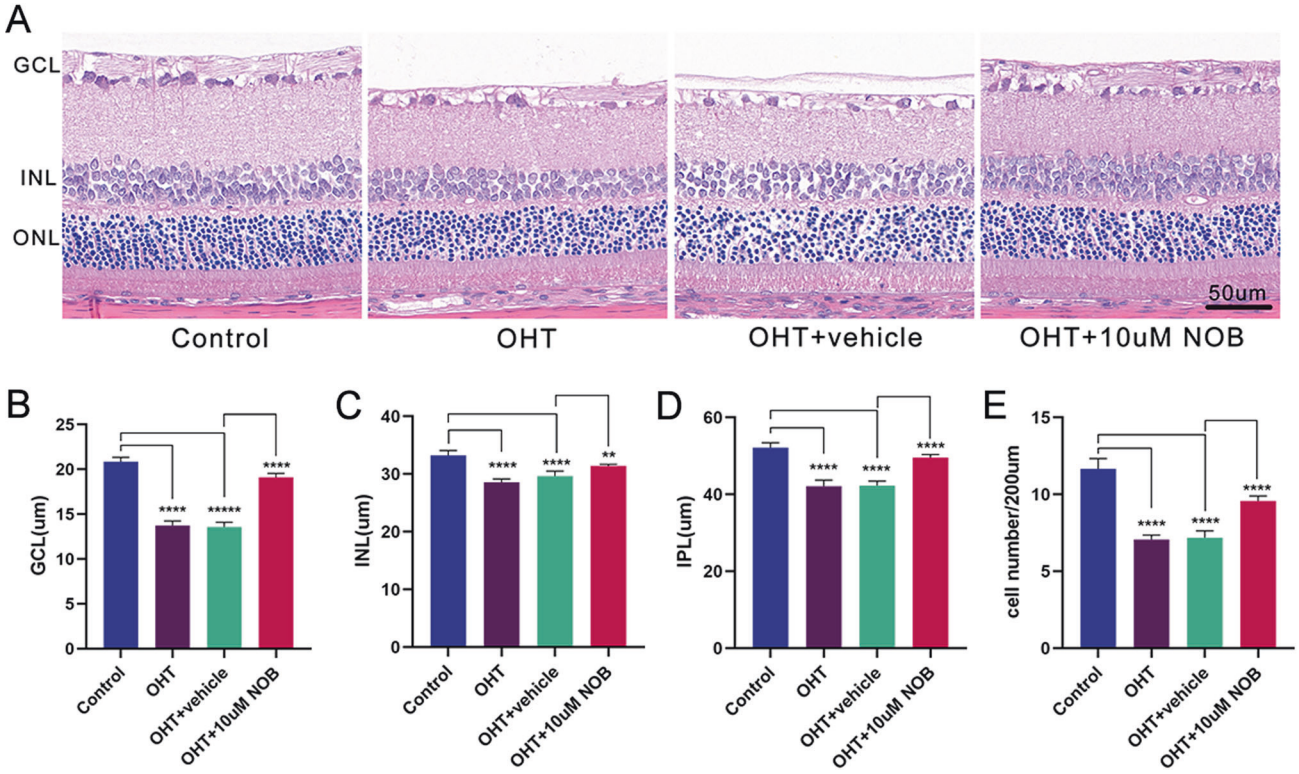

Fig. 5 NOB improves inner retinal structure after 2 weeks of IOP elevation. A Representative H&E staining of retinal sections. Scale bar, 50 μm. **B**–**D** Quantitative analysis of retinal thickness. **E** Quantitative analysis of the number of cells in the GCL. The results are expressed as mean ± SD, $n = 6$. $^{**}P < 0.01$ and $^{****}P < 0.0001$.

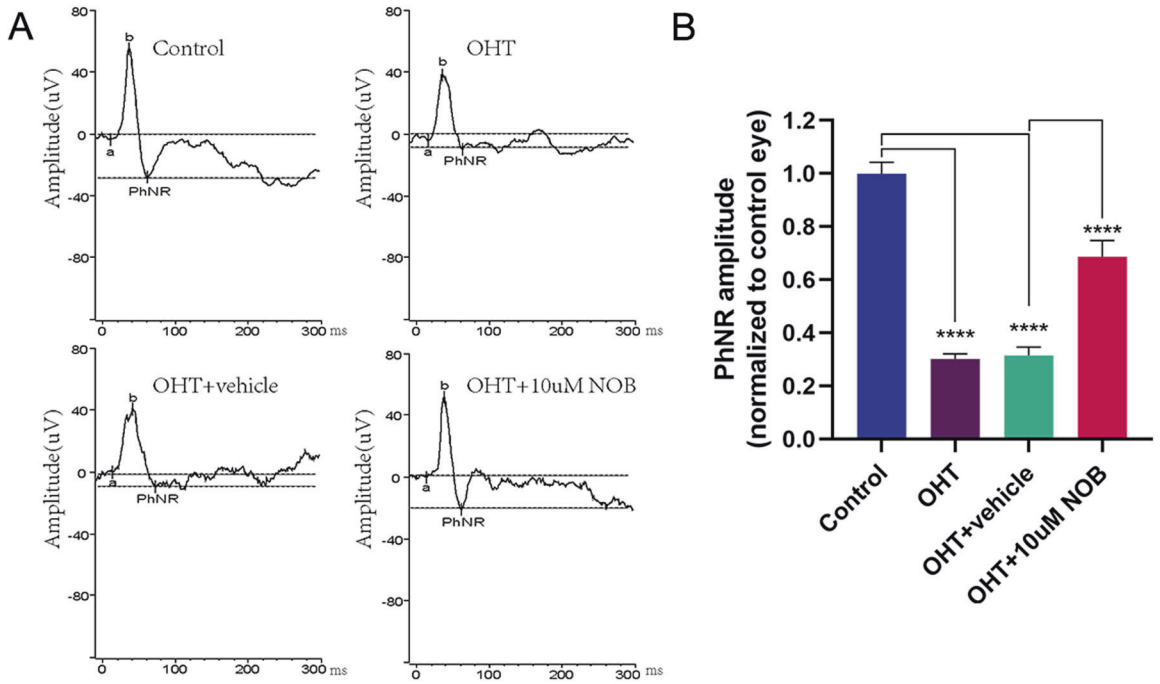

Fig. 6 NOB ameliorates inner retinal dysfunction after 2 weeks of IOP elevation. A Representative PhNR waveforms of retinas in rats with vehicle or 10 μM NOB treatment. **B** Quantification of PhNR amplitude. The results are shown as mean ± SD, $n = 6$. $^{****}P < 0.0001$.

($P < 0.0001$, $n = 6$). With the administration of NOB, a significantly increase of surviving RGCs was observed. In the central region, the density of RGCs increased by 26%, whereas 22% in the middle and 25% in the peripheral region relative to vehicle group (all $P < 0.0001$, $n = 6$). This suggests that NOB promotes RGC survival in this rat models of OHT.

To further demonstrate the protective effect of NOB on RGCs, we performed a TUNEL assay on retinal sections after 2 weeks of

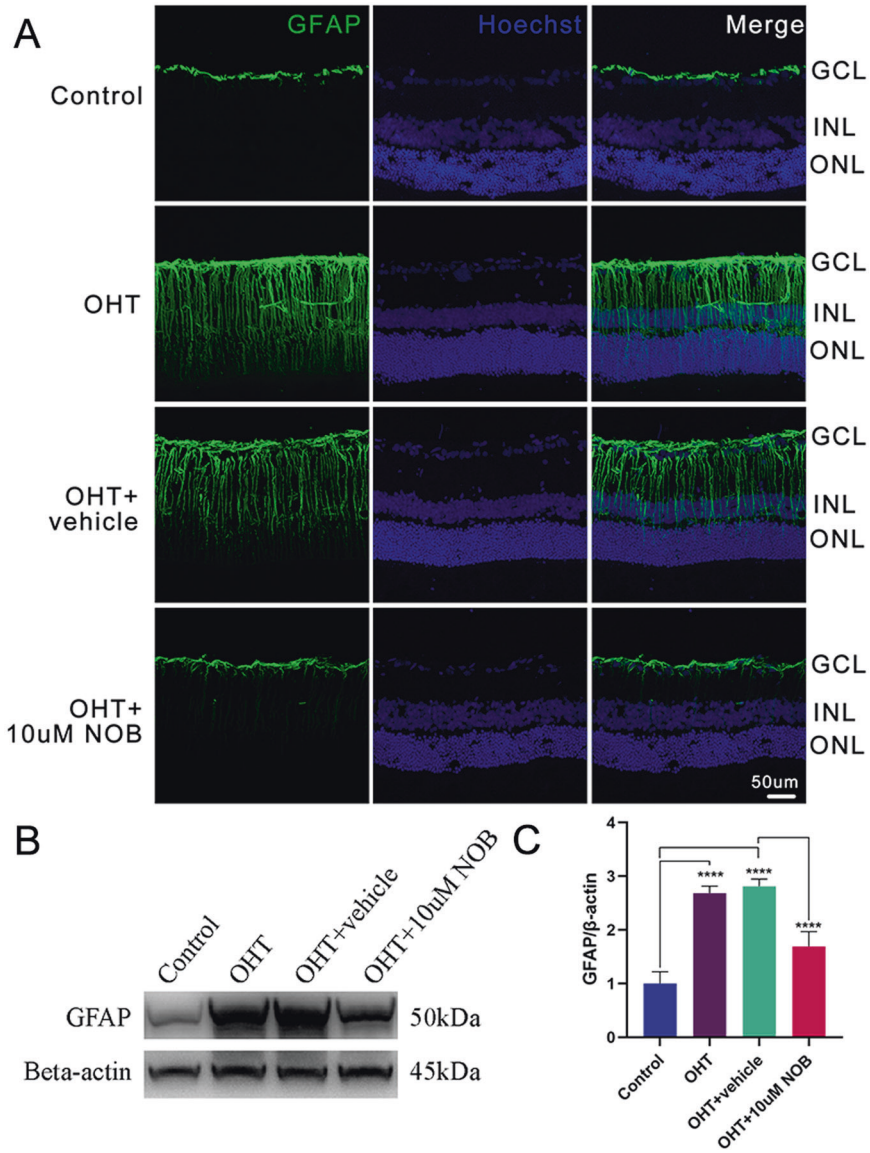

Fig. 7 NOB attenuates Müller glial activation after 2 weeks of IOP elevation. A Immunofluorescence images of retinal sections stained with GFAP and Hoechst 33258. Scale bar, 50 μm. **B** Representative Western blot for GFAP. **C** Quantification of GFAP Western blot normalized to β-actin. The results are expressed as mean ± SD, $n = 6$. ****$P < 0.0001$.

IOP elevation. As shown in Fig. 4, the TUNEL-positive cells in the ganglion cell layer (GCL) were markedly increased in OHT group compared with control group ($P < 0.0001$, $n = 6$), and this change was largely attenuated by the treatment of NOB. Compared with vehicle group, NOB administration significantly decreased the number of TUNEL-positive cells in the GCL ($P < 0.0001$, $n = 6$). Taken together, these results show that NOB alleviates OHT-induced apoptosis of RGCs in this model.

NOB improves inner retinal structure in a rat model of OHT

In this study, we conducted H&E staining on tissue sections to evaluate retinal histological changes in rat models of OHT. Compared with the control, the thickness of inner retina in OHT group was remarkably decreased at 2 weeks post-IOP elevation, while no apparent thinning was observed in outer retina (Fig. 5; $P = 0.0753$ and $P = 0.3448$ for outer nuclear and outer plexiform layer, respectively; $n = 6$). The average thicknesses of control group were 20.87 ± 0.47 μm in the GCL, 33.23 ± 0.84 μm in the inner nuclear layer (INL) and 52.18 ± 1.24 μm in the inner plexiform layer (IPL). After 2 weeks of IOP elevation, the average thicknesses of GCL, INL and IPL were reduced by 34%, 14% and 19%, respectively (all $P < 0.0001$, $n = 6$). In addition, the cellular density in the GCL was 11.67 ± 0.66 cells/200 μm in control group, whereas the density reduced by 39% in OHT group ($P < 0.0001$, $n = 6$). Similar changes were observed in vehicle group. Remarkably, NOB administration partially restored inner retinal structure compared with vehicle group (all $P < 0.01$, $n = 6$). Thus, NOB alleviated OHT-induced inner retinal structural damage, including inner retinal thinning and cell loss in the GCL.

NOB ameliorates inner retinal dysfunction in a rat model of OHT

Increasing evidence indicates that RGC dysfunction often precedes the death in glaucoma[29]. Therefore, there is a critical window of time in which dysfunctional RGCs may be salvaged from irreversible neurodegenerative stages or even recover normal function. Previous research has demonstrated that PhNR is a sensitive marker for inner retinal dysfunction in glaucoma[30]. To determine whether NOB preserves inner retinal function, we measured PhNR at 2 weeks post-surgery. Compared with the

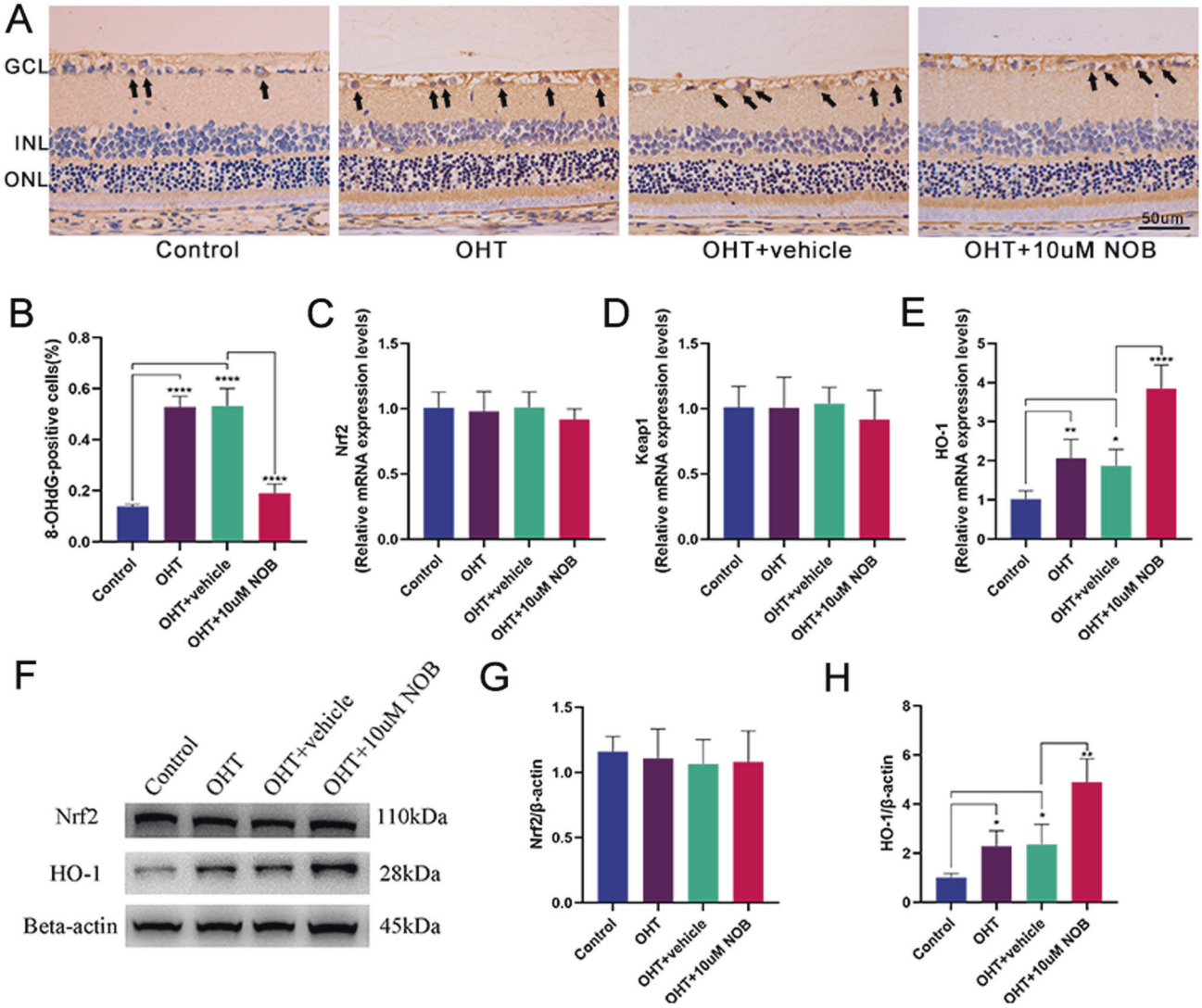

Fig. 8 NOB reduces oxidative stress in RGCs at 2 weeks post-IOP elevation. A Representative immunohistochemical staining of 8-OHdG in retinas from rats with vehicle or 10 μM NOB treatment. Black arrow shows positively stained cells. Scale bar, 50 μm. **B** Quantitative analysis of 8-OHdG-positive cells in the GCL. **C**–**E** Quantification of Nrf2, Keap1 and HO-1 mRNA. **F** Representative Western blot for total Nrf2 and HO-1. **G**, **H** Quantification of total Nrf2 and HO-1 Western blot normalized to β-actin. The results are shown as mean ± SD, $n = 6$. *$P < 0.05$, **$P < 0.01$ and ****$P < 0.0001$.

control, the amplitude of PhNR was markedly reduced by 70% in OHT group (Fig. 6; $P < 0.0001$, $n = 6$). This indicates that high IOP does indeed damage inner retinal function. With the treatment of 10 μM NOB, the decrease of PhNR amplitude was significantly attenuated compared with vehicle group ($P < 0.0001$, $n = 6$). In conclusion, NOB administration helps to ameliorate inner retinal dysfunction in a rat model of OHT, thereby promoting RGC survival.

NOB attenuates Müller glial activation in a rat model of OHT

Müller cells, which are the main glial cells of the retina and span its entire thickness, play a key role in the pathological processes associated with glaucoma[31]. At early stages of glaucoma, Müller cells are activated and produce neurotoxic effects, leading to RGC dysfunction and death[32]. GFAP is not expressed in Müller cells under normal physiological conditions but is upregulated after cell activation[33]. To determine whether NOB attenuates Müller cell activation, we performed immunofluorescence staining and Western blot analysis of GFAP in retinal sections at 2 weeks after surgery. GFAP immunoreactivity was significantly increased in OHT group compared with control group (Fig. 7A); however, NOB significantly reduced the OHT-induced upregulation of GFAP expression. Consistent with this finding, quantification of retinal protein levels by Western blot analysis demonstrated a significant upregulation of GFAP expression at 2 weeks after OHT induction (Fig. 7B, $P < 0.0001$, $n = 6$) and a corresponding attenuation of this change in NOB group ($P < 0.0001$, $n = 6$). These results indicate that NOB attenuates Müller cell activation in this rat model of OHT.

NOB reduces oxidative stress in RGCs in a rat model of OHT

8-OHdG is a marker of oxidative DNA damage and elevated 8-OHdG has been reported in glaucoma[34,35]. To investigate the effect of NOB on oxidative stress in retinas, we performed immunohistochemistry staining of 8-OHdG in retinal sections at 2 weeks after surgery. The number of 8-OHdG-positive cells in the GCL of OHT group was significantly elevated compared with the control (Fig. 8A, B; $P < 0.0001$, $n = 6$); however, this change was significantly attenuated with the administration of 10 μM NOB ($P < 0.0001$, $n = 6$). Thus, NOB reduces OHT-induced oxidative stress in RGCs.

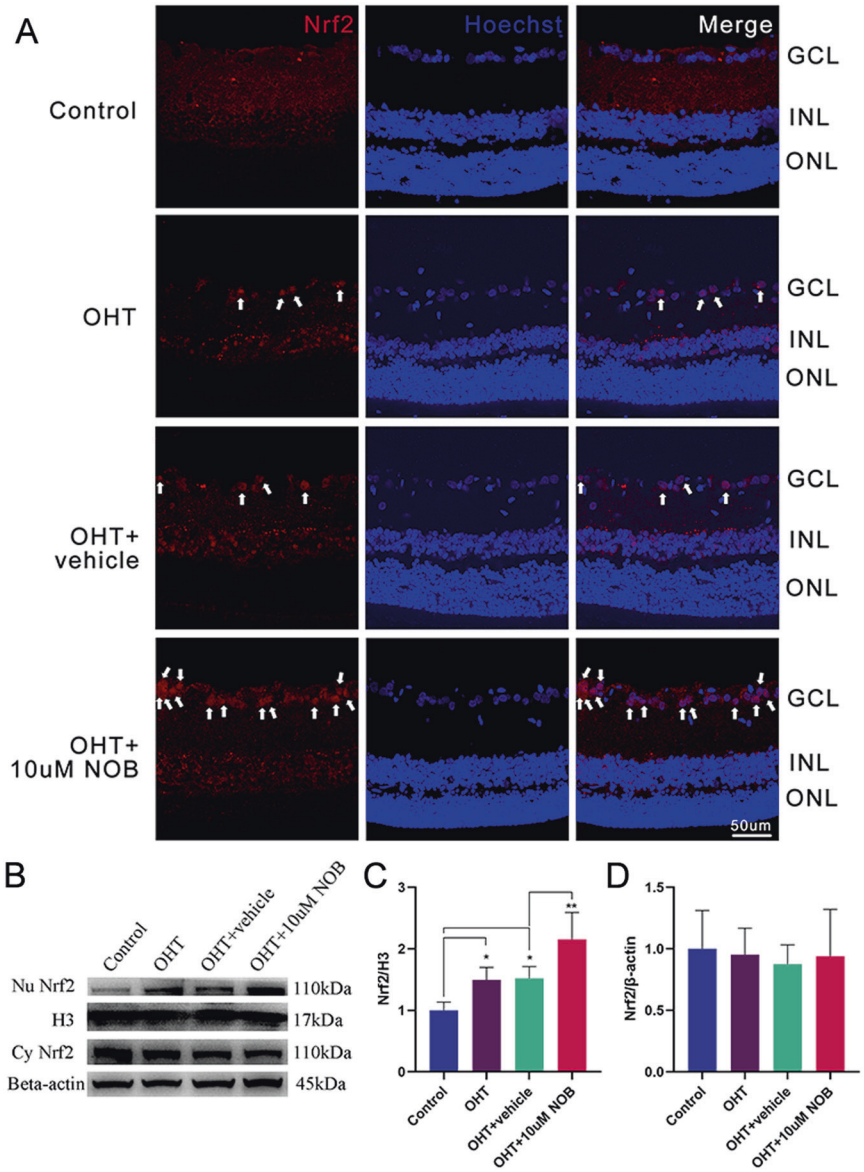

Fig. 9 NOB promotes Nrf2 nuclear translocation and upregulates HO-1 expression in RGCs. A Representative immunofluorescence images of Nrf2 at 2 weeks post-IOP elevation. Scale bar, 50 μm. **B** Representative Western blot for nuclear and cytoplasmic Nrf2. **C** Quantification of nuclear Nrf2 Western blot normalized to H3. **D** Quantification of cytoplasmic Nrf2 Western blot normalized to β-actin. The results are expressed as mean ± SD, $n = 6$. *$P < 0.05$, **$P < 0.01$.

NOB promotes activation of the Nrf2/HO-1 pathway in RGCs in a rat model of OHT

Nrf2 is activated under conditions of oxidative stress and plays a crucial role in regulating the transcription of antioxidant proteins such as HO-1[7]. To determine whether NOB reduces OHT-induced oxidative stress by modulating the Nrf2/HO-1 pathway, we performed quantitative PCR and Western blot analysis of Nrf2 and HO-1 at 2 weeks after surgery (Fig. 8C, E–H). Interestingly, HO-1 expression was elevated at both the mRNA and protein levels of ocular hypertensive rats compared with the control ($P = 0.0031$ and 0.0153, respectively; $n = 6$). Of note, this change was largely enhanced with the administration of NOB ($P < 0.0001$ and 0.0033, respectively; $n = 6$). Keap1 is a negative regulator of Nrf2 and mediates proteasome degradation by binding to Nrf2[6]. However, no significant difference was found in the levels of Nrf2 and Keap1 mRNA among the four groups (Fig. 8D; $P = 0.5282$ and 0.7160, respectively; $n = 6$). Besides, there was no statistical difference in the protein level of total Nrf2 ($P = 0.8446$, $n = 6$).

Previous research has demonstrated that Nrf2 undergoes nuclear translocation in times of oxidative stress. To determine whether NOB upregulates HO-1 expression by promoting Nrf2 nuclear translocation, we conducted immunofluorescence staining of Nrf2. As shown in Fig. 9A, Nrf2 translocation was observed in the GCL after 2 weeks of IOP elevation, and was further enhanced by NOB. For further quantification, we detected the levels of Nrf2 in the nucleus and cytoplasm by Western blot. Similarly, the level of nuclear Nrf2 increased in OHT group at 2 weeks post-IOP elevation ($P = 0.0204$ vs control, $n = 6$). With the treatment of NOB, the expression of nuclear Nrf2 significantly increased compared with vehicle group ($P = 0.0028$, $n = 6$). However, no significant difference was found in the level of cytoplasmic Nrf2 among the four groups ($P = 0.8944$, $n = 6$). This may be related to the sensitivity of the assay. Taken together, NOB enhanced Nrf2 nuclear translocation and its downstream target protein HO-1 expression in RGCs of rats with OHT.

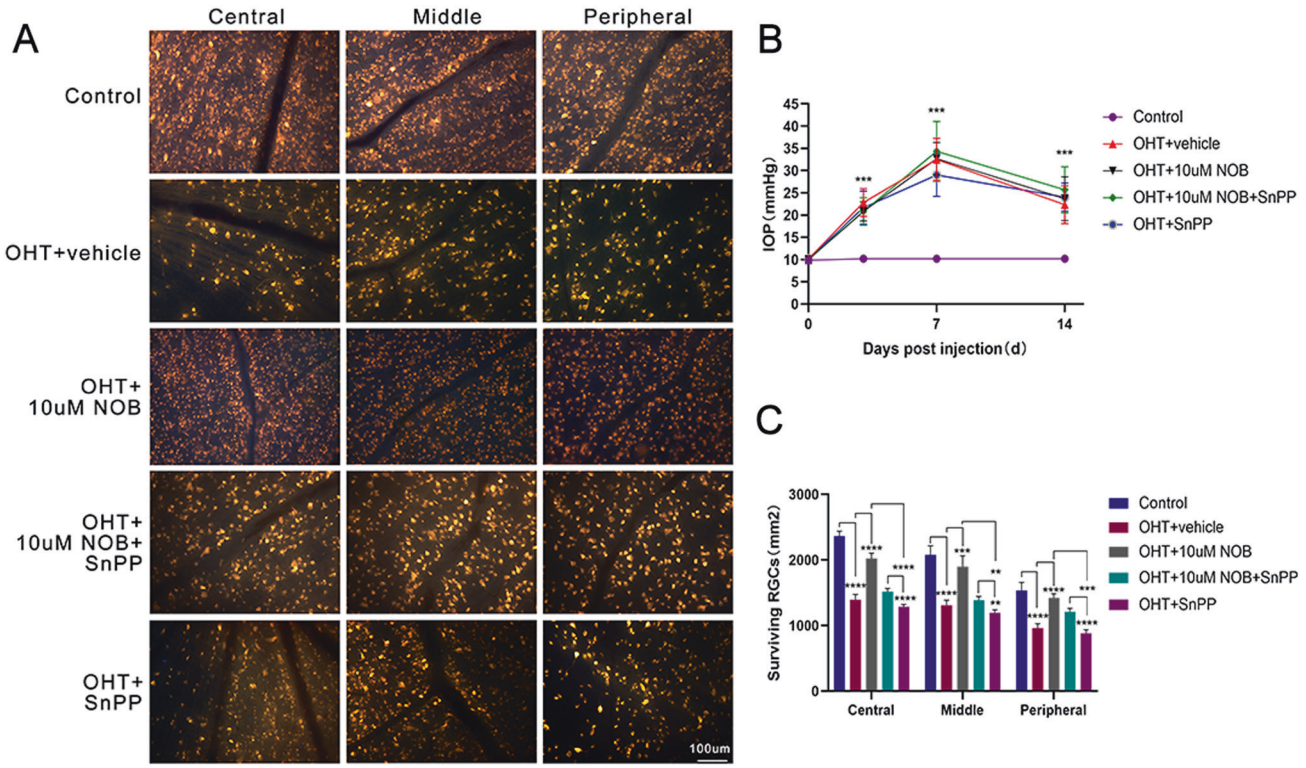

Fig. 10 NOB promotes RGC survival by enhancing Nrf2/HO-1 pathway activation. A Representative images of RGCs labeled with FG. Scale bar, 100 μm. **B** Changes in IOP before surgery and at 3 days, 1 week and 2 weeks after surgery. **C** Quantitative analysis of surviving RGCs. The results are expressed as mean ± SD, $n = 6$. $^{**}P < 0.01$, $^{***}P < 0.001$ and $^{****}P < 0.0001$.

NOB protects RGCs by enhancing Nrf2/HO-1 pathway activation

To investigate whether HO-1 induction by NOB treatment is involved in the neuroprotective role of NOB in rat models of OHT, we performed intravitreal injection of HO-1 inhibitor SnPP. As shown in Fig. 10B, there was no significant difference in IOP level between vehicle group, NOB group, SnPP group and NOB + SnPP group at all indicated time points (all $P > 0.05$, $n = 6$). It suggests that neither NOB nor SnPP have any effect on IOP in this rat model of OHT. Of note, at 2 weeks post-IOP elevation, the average RGC density in NOB + SnPP group significantly decreased compared with NOB group (Fig. 10A, C; $P < 0.0001$, $P = 0.0028$, and $P = 0.0006$ in the central, middle, and peripheral regions, respectively; $n = 6$), but still increased compared with SnPP group ($P < 0.0001$, $P = 0.0011$, and $P < 0.0001$ in the central, middle, and peripheral regions, respectively; $n = 6$). Overall, these results indicate that NOB improves RGC survival in rats with OHT by activating the Nrf2/HO-1 pathway, at least in part.

DISCUSSION

With the aging of the world's population, the prevalence and incidence of glaucoma can be expected to increase. Currently, IOP is the only evidence-based and treatable risk factor for slowing glaucomatous neurodegeneration[2]. However, optic nerve damage may still continue, even if IOP remains in the normal range. Therefore, the importance of neuroprotective drugs is becoming increasingly prominent. Nevertheless, there is no effective neuroprotective drugs for glaucoma. NOB has been shown to have multiple beneficial pharmacological properties, such as anti-inflammatory, anti-aging and anti-diabetic, especially outstanding antioxidant capacity[15]. As a natural compound, its security is guaranteed relative to synthetic compounds[36]. However, the effect of NOB on glaucoma is not clear. To investigate its effect and molecule mechanisms, we established a primary RGCs model of hypoxia in vitro and a rat model of OHT in vivo. Our results first indicate the NOB increases RGC survival both in vivo and in vitro. This effect is achieved in part by attenuating Müller glial activation and improving oxidative stress in RGCs. In addition, it does not depend on IOP lowering.

The pathological process of glaucoma involves a variety of mechanisms, including oxidative stress, glia activation, mitochondrial dysfunction and glutamate excitotoxicity[37]. Müller cells are retina-specific glial cells and span the entire thickness of retinas, while retinal astrocytes are limited to the GCL[32]. Under normal conditions, GFAP is expressed in retinal astrocytes but not by Müller cells; however, reactive Müller cells also express GFAP under pathological conditions[32]. At early stages of glaucoma, Müller cells become reactive and produce neurotoxic effects, along with the upregulation of GFAP, resulting in the neurodegeneration of RGCs[32]. Similarly, we observed an increase of GFAP expression in Müller cells after 2 weeks of IOP elevation. Our results are consistent with studies using other experimental glaucoma models, such as DBA/2 J mice[38], rats treated with laser photocoagulation[28] or cautery of extraocular veins[20]. Notably, NOB attenuated GFAP expression, suggesting the attenuation of Müller glial activation.

In addition, we also found a significant decrease in PhNR amplitude as early as 2 weeks after IOP elevation, which is consistent with previous research[6]. Recent studies suggest this may be related to dendritic pruning and decreased excitability of RGCs[39,40]. RGCs are central nervous system neurons with somas in the inner retina and axons converged on the optic nerve[37]. In glaucoma, RGC dysfunction is usually prior to the onset of irreversible RGCs loss[41]. Thus, PhNR, as a sensitive marker of inner retinal dysfunction, is of great significance for the early diagnosis and monitoring of glaucoma, as demonstrated in several studies[23,42,43]. In this study, NOB administration partially improved

the decline in PhNR amplitude caused by OHT. It is suggested that NOB ameliorates RGC dysfunction, which is significant to slow the progression of glaucomatous neurodegeneration.

Interestingly, we observed an endogenous antioxidant response in retinas of rats with OHT. It was achieved by the activation of Nrf2/HO-1 pathway. However, this compensatory mechanism was insufficient to completely withstand the cumulative damage of OHT. Additionally, a recent study demonstrated that the lack of Nrf2 led to early onset of axonal degeneration and vision loss in experimental glaucoma[6]. Meanwhile, the overexpression of Nrf2 reduced RGC death induced by optic nerve crush[44]. Thus, Nrf2 appears to be a promising therapeutic target for glaucoma. However, in this study, no statistical difference was found in total Nrf2 mRNA or protein levels after 2 weeks of IOP elevation, which is consistent with a previous study[6]. Despite this, we observed the accumulation of Nrf2 immunofluorescence in the nuclei of GCL. This suggests that the endogenous antioxidant response is mediated by Nrf2 nuclear translocation in RGCs. Furthermore, it is further supported by quantification of nuclear Nrf2 protein. HO-1 is a crucial antioxidant enzyme downstream of Nrf2, with the effects of antioxidant, anti-inflammatory and maintaining mitochondrial integrity[45]. Previous research has reported that retinal HO-1 level elevated from 1 to 6 weeks after episcleral vein cauterization[46]. Similarly, HO-1 mRNA and protein levels were increased in retinas at 2 weeks post-IOP elevation in this study. Our observation that the abundance of 8-OHdG-positive GCL cells was increased in retinal sections from rats with OHT is consistent with increasing evidence that oxidative stress plays a crucial role in the pathogenesis of glaucoma[4,5]. We found that NOB reduced 8-OHdG levels and further enhanced activation of the Nrf2/HO-1 pathway in RGCs. This is consistent with the reduction of oxidative damage by NOB in a cerebral ischemia model[47], in cortical neurons stimulated with rotenone[48] and in a toxicity model induced with acetaminophen[49]. Taken together, these results indicate that NOB can activate Nrf2/HO-1 pathway in RGCs to further support the antioxidant defense of RGCs under conditions of OHT, thus exerting an outstanding neuroprotective role.

In conclusion, we first demonstrate that NOB has significant neuroprotective effects on RGCs, including reducing RGC apoptosis and oxidative stress, partially restoring RGC dysfunction, further enhancing Nrf2/HO-1 pathway in RGCs, and attenuating Müller glial activation. These effects do not depend on IOP lowering. Interventions to enhance activation of Nrf2/HO-1 pathway are viable therapies for glaucoma.

DATA AVAILABILITY

The data that support the findings of this study are available from the corresponding author on reasonable request.

REFERENCES

1. Sun XH, Dai Y, Chen YH, Yu DY, Cringle SJ, Chen JY, et al. Primary angle closure glaucoma: what we know and what we don't know. Progress in Retinal and Eye Research 57, 26–45 (2017).
2. Storgaard L, Tran TL, Freiberg JC, Hauser AS, Kolko M. Glaucoma Clinical Research: Trends in Treatment Strategies and Drug Development. Front Med (Lausanne) 8,733080 (2021).
3. Killer HE, Pircher A. Normal tension glaucoma: review of current understanding and mechanisms of the pathogenesis. Eye (Lond) 32,924–930 (2018).
4. Caceres-Velez PR, Hui F, Hercus J, Bui B, Jusuf PR. Restoring the oxidative balance in age-related diseases - An approach in glaucoma. Ageing Res Rev 75,101572 (2022).
5. Kang EY, Liu PK, Wen YT, Quinn PMJ, Levi SR, Wang NK, et al. Role of Oxidative Stress in Ocular Diseases Associated with Retinal Ganglion Cells Degeneration. Antioxidants (Basel) 10,(2021).
6. Naguib S, Backstrom JR, Gil M, Calkins DJ, Rex TS. Retinal oxidative stress activates the NRF2/ARE pathway: An early endogenous protective response to ocular hypertension. Redox Biol 42, 101883 (2021).
7. Wang M, Li J, Zheng Y. The Potential Role of Nuclear Factor Erythroid 2-Related Factor 2 (Nrf2) in Glaucoma: A Review. Med Sci Monit 26,e921514 (2020).
8. Zhang Q, Liu J, Duan H, Li R, Peng W, Wu C. Activation of Nrf2/HO-1 signaling: An important molecular mechanism of herbal medicine in the treatment of atherosclerosis via the protection of vascular endothelial cells from oxidative stress. J Adv Res 34,43–63 (2021).
9. Matsuzaki K, Ohizumi Y. Beneficial Effects of Citrus-Derived Polymethoxylated Flavones for Central Nervous System Disorders. Nutrients 13,(2021).
10. Li SY, Li X, Chen FY, Liu M, Ning LX, Yan YF, et al. Nobiletin mitigates hepatocytes death, liver inflammation, and fibrosis in a murine model of NASH through modulating hepatic oxidative stress and mitochondrial dysfunction dagger. J Nutr Biochem 100,(2022).
11. Miyata Y, Matsumoto K, Kusano S, Kusakabe Y, Katsura Y, Oshitari T, et al. Regulation of Endothelium-Reticulum-Stress-Mediated Apoptotic Cell Death by a Polymethoxylated Flavone, Nobiletin, Through the Inhibition of Nuclear Translocation of Glyceraldehyde 3-Phosphate Dehydrogenase in Retinal Muller Cells. Cells 10,(2021).
12. Qi G, Mi Y, Fan R, Li R, Liu Z, Liu X. Nobiletin Protects against Systemic Inflammation-Stimulated Memory Impairment via MAPK and NF-kappaB Signaling Pathways. J Agric Food Chem 67,5122–5134 (2019).
13. Nohara K, Mallampalli V, Nemkov T, Wirianto M, Yang J, Ye Y, et al. Nobiletin fortifies mitochondrial respiration in skeletal muscle to promote healthy aging against metabolic challenge. Nat Commun 10,3923 (2019).
14. Wirianto M, Wang CY, Kim E, Koike N, Gomez-Gutierrez R, Nohara K, et al. The clock modulator Nobiletin mitigates astrogliosis-associated neuroinflammation and disease hallmarks in an Alzheimer's disease model. FASEB J 36,e22186 (2022).
15. Nakajima A, Ohizumi Y. Potential Benefits of Nobiletin, A Citrus Flavonoid, against Alzheimer's Disease and Parkinson's Disease. Int J Mol Sci 20,(2019).
16. Gao F, Li T, Hu J, Zhou X, Wu J, Wu Q. Comparative analysis of three purification protocols for retinal ganglion cells from rat. Mol Vis 22,387–400 (2016).
17. Hu X, Dai Y, Sun X. Parkin overexpression protects retinal ganglion cells against glutamate excitotoxicity. Mol Vis 23,447–456 (2017).
18. Samsel PA, Kisiswa L, Erichsen JT, Cross SD, Morgan JE. A Novel Method for the Induction of Experimental Glaucoma Using Magnetic Microspheres. Invest Ophth Vis Sci 52,1671–1675 (2011).
19. Huang WJ, Gao FJ, Hu FY, Huang JC, Wang M, Xu P, et al. Asiatic Acid Prevents Retinal Ganglion Cell Apoptosis in a Rat Model of Glaucoma. Front Neurosci-Switz 12,(2018).
20. Zhang X, Zhang R, Zhou X, Wu J. Decreased d-Serine Levels Prevent Retinal Ganglion Cell Apoptosis in a Glaucomatous Animal Model. Invest Ophthalmol Vis Sci 59,5045–5052 (2018).
21. Naskar R, Wissing M, Thanos S. Detection of early neuron degeneration and accompanying microglial responses in the retina of a rat model of glaucoma. Invest Ophthalmol Vis Sci 43,2962–2968 (2002).
22. Kasnak G, Firatli E, Kononen E, Olgac V, Zeidan-Chulia F, Gursoy UK. Elevated levels of 8-OHdG and PARK7/DJ-1 in peri-implantitis mucosa. Clin Implant Dent Relat Res 20,574–582 (2018).
23. Chrysostomou V, Crowston JG. The photopic negative response of the mouse electroretinogram: reduction by acute elevation of intraocular pressure. Invest Ophthalmol Vis Sci 54,4691–4697 (2013).
24. Zhang X, Zhang R, Chen J, Wu J. Neuroprotective effects of DAAO are mediated via the ERK1/2 signaling pathway in a glaucomatous animal model. Exp Eye Res 190,107892 (2020).
25. Zhao Y, Sun Y, Wang G, Ge S, Liu H. Dendrobium Officinale Polysaccharides Protect against MNNG-Induced PLGC in Rats via Activating the NRF2 and Antioxidant Enzymes HO-1 and NQO-1. Oxid Med Cell Longev 2019, 9310245 (2019).
26. Jassim AH, Fan Y, Pappenhagen N, Nsiah NY, Inman DM. Oxidative Stress and Hypoxia Modify Mitochondrial Homeostasis During Glaucoma. Antioxid Redox Signal 35,1341–1357 (2021).
27. Vernazza S, Oddone F, Tirendi S, Bassi AM. Risk Factors for Retinal Ganglion Cell Distress in Glaucoma and Neuroprotective Potential Intervention. Int J Mol Sci 22,(2021).
28. Dai Y, Hu X, Sun X. Overexpression of parkin protects retinal ganglion cells in experimental glaucoma. Cell Death Dis 9,88 (2018).
29. Porciatti V, Chou TH. Modeling Retinal Ganglion Cell Dysfunction in Optic Neuropathies. Cells 10,(2021).
30. Tang J, Hui F, Hadoux X, Soares B, Jamieson M, van Wijngaarden P, et al. Short-Term Changes in the Photopic Negative Response Following Intraocular Pressure Lowering in Glaucoma. Invest Ophthalmol Vis Sci 61,16 (2020).
31. Xue B, Xie Y, Xue Y, Hu N, Zhang G, Guan H, et al. Involvement of P2X7 receptors in retinal ganglion cell apoptosis induced by activated Muller cells. Exp Eye Res 153,42–50 (2016).

32. Shinozaki Y, Koizumi S. Potential roles of astrocytes and Muller cells in the pathogenesis of glaucoma. J Pharmacol Sci 145,262–267 (2021).
33. Woldemussie E, Wijono M, Ruiz G. Muller cell response to laser-induced increase in intraocular pressure in rats. Glia 47,109–119 (2004).
34. Himori N, Kunikata H, Shiga Y, Omodaka K, Maruyama K, Takahashi H, et al. The association between systemic oxidative stress and ocular blood flow in patients with normal-tension glaucoma. Graefes Arch Clin Exp Ophthalmol 254,333–341 (2016).
35. Wang X, Ng YK, Tay SS. Factors contributing to neuronal degeneration in retinas of experimental glaucomatous rats. J Neurosci Res 82,674–689 (2005).
36. Kesharwani SS, Mallya P, Kumar VA, Jain V, Sharma S, Dey S. Nobiletin as a Molecule for Formulation Development: An Overview of Advanced Formulation and Nanotechnology-Based Strategies of Nobiletin. Aaps Pharmscitech 21,(2020).
37. Almasieh M, Wilson AM, Morquette B, Cueva Vargas JL, Di Polo A. The molecular basis of retinal ganglion cell death in glaucoma. Prog Retin Eye Res 31,152–181 (2012).
38. Inman DM, Horner PJ. Reactive nonproliferative gliosis predominates in a chronic mouse model of glaucoma. Glia 55,942–953 (2007).
39. Risner ML, Pasini S, Cooper ML, Lambert WS, Calkins DJ. Axogenic mechanism enhances retinal ganglion cell excitability during early progression in glaucoma. Proc Natl Acad Sci U S A 115,E2393–E2402 (2018).
40. Pang JJ, Frankfort BJ, Gross RL, Wu SM. Elevated intraocular pressure decreases response sensitivity of inner retinal neurons in experimental glaucoma mice. Proc Natl Acad Sci U S A 112,2593–2598 (2015).
41. Fry LE, Fahy E, Chrysostomou V, Hui F, Tang J, van Wijngaarden P, et al. The coma in glaucoma: Retinal ganglion cell dysfunction and recovery. Prog Retin Eye Res 65,77–92 (2018).
42. Prencipe M, Perossini T, Brancoli G, Perossini M. The photopic negative response (PhNR): measurement approaches and utility in glaucoma. Int Ophthalmol 40,3565–3576 (2020).
43. Machida S. Clinical applications of the photopic negative response to optic nerve and retinal diseases. J Ophthalmol 2012,397178 (2012).
44. Fujita K, Nishiguchi KM, Shiga Y, Nakazawa T. Spatially and Temporally Regulated NRF2 Gene Therapy Using Mcp-1 Promoter in Retinal Ganglion Cell Injury. Mol Ther-Meth Clin D 5,130–141 (2017).
45. Chiang SK, Chen SE, Chang LC. The Role of HO-1 and Its Crosstalk with Oxidative Stress in Cancer Cell Survival. Cells 10, (2021).
46. Wang X, Yuan ZL. Activation of Nrf2/HO-1 pathway protects retinal ganglion cells from a rat chronic ocular hypertension model of glaucoma. Int Ophthalmol 39,2303–2312 (2019).
47. Zhang L, Zhang X, Zhang C, Bai X, Zhang J, Zhao X, et al. Nobiletin promotes antioxidant and anti-inflammatory responses and elicits protection against ischemic stroke in vivo. Brain Res 1636, 130–141 (2016).
48. Amarsanaa K, Kim HJ, Ko EA, Jo J, Jung SC. Nobiletin Exhibits Neuroprotective Effects against Mitochondrial Complex I Inhibition via Regulating Apoptotic Signaling. Exp Neurobiol 30,73–86 (2021).
49. Guvenc M, Cellat M, Gokcek I, Ozkan H, Arkali G, Yakan A, et al. Nobiletin attenuates acetaminophen-induced hepatorenal toxicity in rats. J Biochem Mol Toxicol 34,e22427 (2020).

AUTHOR CONTRIBUTIONS

DDW, FJG, XJZ and JHW conceived and designed the study. DDW, XJZ, FYH and PX conducted experiments. DDW and FJG performed data analysis. DDW and JHW contributed to the writing of the manuscript. All authors approved the final version to be published.

FUNDING

This work was supported by the grants from the National Natural Science Foundation of China (No. 81770925, 81790641), Outstanding academic leaders in Shanghai (20XD1401100), Program for Outstanding Medical Academic Leader (2019LJ01) and the Non-profit Central Research Institute Fund of Chinese Academy of Medical Sciences (2018PT32019).

COMPETING INTERESTS

The authors declare no competing interests.

ETHICS APPROVAL

All animal experiments were approved by the Animal Experimental Ethics Committee of the Eye and ENT Hospital of Fudan University.

ADDITIONAL INFORMATION

Correspondence and requests for materials should be addressed to Ji-Hong Wu.